Научном већу
Института за физику
Прегревица 118, Земун

Предмет: Реизбор у звање истраживач сарадник

Молим Научно веће Института за физику да покрене поступак за мој реизбор у звање истраживач сарадник.

Прилажем:

- Мишљење руководиоца пројекта
- Биографију
- Преглед научне активности
- Списак научних радова
- Копије научних радова
- Потврду о завршеним основним академским студијама
- Копију дипломе основних академских студија
- Потврду о упису на докторске академске студије
- Уверење о положеним испитима на докторским студијама
- Доказ о одбрањеној теми пред Колегијумом докторских студија

С поштовањем,

Душан Грујић
Душан Грујић

Мишљење руководиоца пројекта

ИНСТИТУТ ЗА ФИЗИКУ
ПРИМЉЕНО: 31. 10. 2019

Рад.јед.	број	Арх.шифра	Прилог
0801	1638/2		

Молим Научно веће Института за физику

да покрене поступак за реизбор Душана Грујића у звање истраживач сарадник. Колега Грујић је уписан на Докторске академске студије на Физичком факултету, Универзитета у Београду, смер Фотоника и ласери. Учествовао је у изради осам радова у међународним часописима. Колега Грујић ангажован је на пројекту ИИИ 45016 Министарства просвете, науке и технолошког развоја "Генерисање и карактеризација нанофотонских функционалних структура у биомедицини". Резултати које је постигао колега Грујић показују да поседује неопходне способности за израду докторске дисертације, као и да се активно бави научно-истраживачким радом. Овим наведеним, колега задовољава све неопходне услове Министарства просвете, науке и технолошког развој за реизбор у звање истраживач сарадник. За чланове Комисије у поступку реизбора предлажем:

- др Бранислава Јеленковића - научни саветник, Институт за физику у Београду
- др Дејана Пантелића - научни саветник, Институт за физику у Београду
- др Зорана Николића – ванредни професор, Физички факултет у Београду

Уз поштовање,

Руководилац пројекта ИИИ 45016 Министарства просвете, науке и технолошког развоја

Научни саветник Института за физику,

др Бранислав Јеленковић

Биографија кандидата

Душан Грујић је рођен у Крушевцу, Република Србија, 24.02.1984. године. У Крушевцу је завршио основну школу и Гимназију, природно – математички смер. 2010. године дипломира (основне академске студије) на Физичком факултету, Универзитета у Београду, смер Примењена физика и информатика са просечном оценом 8,14. Дипломски рад је одбранио на тему „Примена нумеричких метода у анализама Cole-Cole дијаграма". Од 01.01. 2011. године је запослен у Институту за физику, са ангажовањем на пројекту Министарства просвете, науке и технолошког развоја "Генерисање и карактеризација нанофотонских функционалних структура у биомедицини и информатици". Од јануара 2012. године је уписан на Докторске академске студије Физичког факултета Универзитета у Београду, смер Фотоника и ласери и тренутно је на трећој години. На састанку Колегијума докторских студија Физичког факултета 18.09.2019 прихваћена је тема кандидата са насловом: Примена дигиталне холографије за детекцију инфрацрвеног зрачења на биофотонским структурама. До сада је публиковао три научна рада у часопису категорије М21, три научна рада у часопису категорије М22 и два категорије М23. Резултати истраживања представљени су на преко десет конференција. Поред тога, поднета је и патентна пријава Заводу за интелектуалну својину Републике Србије.

Преглед научне активности

Душан Грујић је био ангажован као истраживач на реализацији уређаја за формирање тзв. дот-матрикс холограма. Због специфичности начина уписивања оваквих холограма на фоторегиструјући материјал потребна је координација свих елемената на уређају, то јест усаглашен рад механичких и оптичких елемената, те је доста рађено на унапређењу комуникације софтвера са опремом која служи за позиционирање одговарајуће оптике, као и самог материјала на коме се врши уписивање дијаграма. Касније је ова апаратура надограђена тако да се на њој могу ласерским снопом генерисати оптички индуковане фотонске структуре у нелинеарном медијуму. Као нелинеарни медијум је коришћен литијум-ниобат допиран гвожђем, у облику танког правоугаоног блока (апроксимација једнодимензионе структуре). Струтуре су реализоване у виду низа таласовода који су уписивани интензивним ласерским зрачењем нормалним на површину блока, при чему се исти помера аутоматским дводимензионим позиционером. Ова мултифункционална апаратура може служити и за фабрикацију миркосочива, биомиметичких структура, а у плану је надоградња исте тако да може служити и као дигитални холографски миркоскоп.

Научна активност Душана Грујића је примарно базирана на експериментима који се тичу дигиталне холографије и њене примене на мерење структура и деформација малих димензија. За потребе ових експеримената је учествовао у развијању холографске методе снимања објеката у више димензија. То подразумева израду специфичне експерименталне поставке којом се обезбеђује квалитетније прикупљање информација о снимaном објекту , као и израду софтвера којим се врши снимање и нумеричка реконструкција дигиталног холограма Френеловом трансформацијом где је за убрзавање целокупног процеса обраде уведено коришћење NVIDIA графичких картица и CUDA протокола паралелног процесирања. Холограм се региструје директно на CCD чип камере која је повезана са рачунаром на ком се складиште подаци и веома брзо извршава обрада захваљујући паралелном процесирању. На овај начин је остварена уштеда у времену и материјалу у односу на аналогни начин обраде који се користио раније. Такође, могуће је један исти холограм реконструисати више пута (што код аналогне није могуће), са различитим нумеричким параметрима у циљу добијања што боље реконструкције. Коришћењем метода холографске интерферометрије могу се добити информације о деформацији, снимањем и упоређивањем два холограма истог објекта у различитим условима. Обзиром да се у поставци експеримента користи сферно огледало, слика која се добија је у већини случајева закривљена. Знајући параметре огледала и користећи могућност пропагације уназад, део кода за аутоматску корекцију слике је успешно имплементиран. Грујић ради на новом начину детекције зрачења који је примењив у веома широком спектралном интервалу - од ултраљубичастог, преко видљивог и инфрацрвеног, до терахерцног зрачења. Коришћењем вештачки произведених порозних материјала била би могућа реализација и пикселизованог сензора – камере. Већ у иницијалним експериментима постигнута је осетљивост детекције поредива са комерцијалним термалним камерама. Даљим усавршавањем очекује се значајно повећање осетљивости, а самим тим и примењивости оваквих детектора.

Радови након претходног избора у звање

Радови у врхунским међународним часописима - категорија M21:

(1) **Dusan Grujic**, Darko Vasiljevic, Dejan Pantelic, Ljubisa Tomic, Zoran Stamenkovic, and Branislav Jelenkovic, Infrared camera on a butterfly's wing, *Optics Express*, vol. 26, no. 11, pp. 14143-14158, (2018) ISSN 1094-4087, DOI: 10.1364/OE.26.014143

Радови у истакнутим међународним часописима - категорија M22:

(1) Svetlana Savić-Šević, Dejan Pantelić, **Dušan Grujić**, Branislav Jelenković, Localization of light in a polysaccharide-based complex nanostructure, *Opt Quant Electron* 48: 289. (2016), ISSN 0306-8919, DOI:10.1007/s11082-016-0560-8

Саопштење са међународног скупа штампано у изводу - категорија M34:

(1) M. Simovic-Pavlovic, **D. Grujic**, P. Atanasijevic, D. Vasiljevic, B. Kolaric and D. Pantelic, Measuring temperature changes of butterfly's wing through deformation: a holographic approach, *Photonica 2019, VII International School and Conference on Photonics, Belgrade, Serbia, 26 August - 30 August 2019*
(2) M. Spasenovic, J. Mitric, D. Abramovic, N. Demoli, **D. Grujic**, D. Pantelic, I. Salom, D. Todorovic, Graphene acoustic diaphragms, *Photonica 2017 - The 6th International School and Conference on Photonics, Belgrade, Serbia, 28 August - 1 September 2017*
(3) J. Mitric, **D. Grujic**, D. Abramovic, D. Todorovic, I. Salom, N. Demoli, D. Pantelic, M. Spasenovic, Digital holography of graphene oxide paper acoustic membranes, *Photonica 2017 - The 6th International School and Conference on Photonics, Belgrade, Serbia, 28 August - 1 September 2017*
(4) J. Mitric, **D. Grujic**, D. Abramovic, I. Salom, N. Demoli, D. Pantelic, D. Todorovic, M. Spasenovic, Digital holography of graphene paper acoustic membranes and comparison to other paper - like materials, *Sixteenth Young Researches Conference - Materials Science and Engineering, Institute of Technical Sciences of SASA, isbn: 978-86-80321-33-2, Belgrade, 6. - 8. Dec, 2017*

Радови пре претходног избора у звање:

(1) Dejan V. Pantelić, **Dušan Ž. Grujić**, Darko M. Vasiljević, Single-beam, dual-view digital holographic interferometry for biomechanical strain measurements of biological objects, *J. Biomed. Opt.* 19(12), 127005 (2014), ISSN 1083-3668, DOI:10.1117/1.JBO.19.12.127005, IF= 2.859, M21

(2) D Pantelić, S Savić-Šević and **D Grujić**, Zoom system for measurement of coherent backscattering of light in micro- and nanomaterials, *Physica Scripta T* 157 014020 (2013), ISSN 0031-8949, DOI: 10.1088/0031-8949/2013/T157/014020, IF= 1.186, M22

(3) Boban Zarkov, **Dušan Grujić** and Dejan Pantelić, High-resolution dot-matrix hologram generation, *Physica Scripta T* 149 014021 (2012), ISSN 0031-8949, DOI: 10.1088/0031-8949/2012/T149/014021, IF= 1.024, M22

(4) N. M. Lučić, D. M. Jović Savić, A. Piper, **D. Ž. Grujić**, J. M. Vasiljević, D. V. Pantelić, B. M. Jelenković, and D. V. Timotijević, Light propagation in quasiperiodic Fibonacci waveguide arrays, *J. Opt. Soc. Am. B* 32 7 1510 (2015), ISSN 0740-3224, DOI: 10.1364/JOSAB.32.001510, IF= 1.695, M22

(5) N. M. Lučić, B. M. Bokić, **D. Ž. Grujić**, D. V. Pantelić, B. M. Jelenković, A. Piper, D. M. Jović, and D. V. Timotijević, Defect-guided Airy beams in optically induced waveguide arrays, *Phys. Rev. A* 88, 063815 (2013), ISSN 1050-2947, DOI: 10.1103/PhysRevA.88.063815, IF= 2.991, M21

(6) Svetlana Savic-Sevic, Dejan Pantelic, **Dusan Grujic**, Branislav Jelenkovic, Srecko Curcic, Bozidar Curcic, Dejan Stojanovic, Localization of light in photonic crystals of biological origin, ICTON 2012 : 14th International Conference on Transparent Optical Networks, pp. 1 - 3, issn: 978-1-4673-2228-7, doi: 10.1109/ICTON.2012.6253864, United Kingdom, 1.-4. Jul, 2012, M31

(7) N. M. Lucic, B. M. Bokic, **D. Z. Grujic**, Dejan Pantelic, Branislav Jelenkovic, A. Piper, D. M. Jovic, and D. V. Timotijevic, Guiding of Airy beams with optically induced waveguide arrays in the nonlinear crystal, Transparent Optical Networks (ICTON), 2014 16th International Conference on, IEEE, vol. 1, no. 1, pp. 1 - 3, issn: 14526553, doi: 10.1109/ICTON.2014.6876684, Austria, 5.-9. Jul, 2014, M31

(8) B. Muric, **D. Grujic**, D. Milovanovic, D. Pantelic, D. Vasiljevic and B. Jelenkovic, Fast fabrication of large area concave microlens arrays, 12th International Conference on Fundamental and Applied Aspects of Physical Chemistry, Physical Chemistry 2014, Society of Physical Chemists of Serbia, pp. 711 - 714, issn: 978-86-82475-31-6, Serbia, 21. - 25. Sep, 2014, M33

(9) J. Mitric, **D. Grujic**, D. Abramovic, N. Demoli, D. Pantelic, I. Salom, D. Todorovic, M. Spasenovic, Digitalna holografija akustickih membrana od grafenskog papira, Proceedings of the Fourth International Acoustics and Audio Engineering Conference TAKTONS 2017, Fakultet tehnickih nauka, Novi Sad, pp. 38 - 41, isbn: 978-86-7892-994-6, Novi Sad, Srbija, 22. - 25. Nov, 2017, M33

(10) J. Vasiljevic, N. M. Lucic, D. V. Timotijevic, A. Piper, **D. Z. Grujic**, D. Pantelic, B. Jelenkovic, D. M. Jovic Savic, Light propagation in deterministic aperiodic Fibonacci waveguide arrays, Photonica 2015, V International School and Conference on Photonics, Vinca Institute of Nuclear Sciences, pp. 74 - 75, issn: 978-86-7306-131-3, Srbija, 23. - 27. Aug, 2015, M34

(11) **D.Z. Grujic**, D. Vasiljevic, D. Pantelic, Dental composite polymerization process: digital holographic interferometry method, Photonica 2015, V International School and Conference on Photonics, Vinca Institute of Nuclear Sciences, pp. 182 - 183, issn: 978-86-7306-131-3, Srbija, 23. - 27. Aug, 2015, M34

(12) N. M. Lucic, B. M. Bokic, **D. Z. Grujic**, D. Pantelic, B. Jelenkovic, A. Piper, D. Jovic, D. Timotijevic, Airy beam propagation along one dimensional optically induced photonic lattice with defect, Oasis 5th Conference and Exhibition on Optics and Electro-Optics, MEDINANO, pp. 74, Israel, 3. - 4. Mar, 2015, M34

(13) N. Lucic, B. Bokic, **D. Grujic**, D. Pantelic, B. Jelenkovic, J. Vasiljevic, D. Timotijevic, A. Piper, D. Jovic Savic, Defect controlled Airy beam acceleration in optically induced waveguide arrays, PHOTONICA 2013, IV International School and Conference on Photonics, isbn: 978-86-82441-36-6, Beograd, Srbija, 25. - 29. Aug, 2013, M34

(14) D. Pantelic, **D. Grujic**, J. Vasiljevic, Prakticne primene digitalne holografije, Konferencija sesta radionica fotonike - Zbornik apstrakata, pp. 8 - 8, isbn: 978-86-82441-35- 9, Kopaonik, 4. - 8. Mar, 2013, M64

Research Article
Vol. 26, No. 11 | 28 May 2018 | OPTICS EXPRESS 14143
Optics EXPRESS

Infrared camera on a butterfly's wing

DUŠAN GRUJIĆ,[1,*] DARKO VASILJEVIĆ,[1] DEJAN PANTELIĆ,[1] LJUBIŠA TOMIĆ,[2] ZORAN STAMENKOVIĆ,[3] AND BRANISLAV JELENKOVIĆ[1]

[1]*Institute of Physics Belgrade, University of Belgrade, Photonics Center, Pregrevica 118, 11080 Zemun, Belgrade, Serbia*
[2]*Military Technical Institute, Ratka Resanovića 1, 11030 Belgrade, Serbia*
[3]*Faculty of Mechanical Engineering, University of Niš, Department for Production and Information Technology, Laboratory for Intelligent Manufacturing Systems, Aleksandra Medvedeva 14, 18000 Niš, Serbia*
**dusang@ipb.ac.rs*

Abstract: Thermal cameras were constructed long ago, but working principles and complex technologies still limit their resolution, total number of pixels, and sensitivity. We address the problem of finding a new sensing mechanism surpassing existing limits of thermal radiation detection. Here we reveal the new mechanism on the butterfly wing, whose wing-scales act as pixels of an imaging array on a thermal detector. We observed that the tiniest features of a *Morpho* butterfly wing-scale match the mean free path of air molecules at atmospheric pressure – a condition when the radiation-induced heating produces an additional, thermophoretic force that deforms the wing-scales. The resulting deformation field was imaged holographically with mK temperature sensitivity and 200 Hz response speed. By imitating butterfly wing-scales, the effect can be further amplified through a suitable choice of material, working pressure, sensor design, and detection method. The technique is universally applicable to any nano-patterned, micro-scale system in other spectral ranges, such as UV and terahertz.

OCIS codes: (040.3060) Infrared detectors; (110.3080) Infrared imaging; (350.5340) Photothermal effects; (090.1995) Digital holography.

References and links

1. A. Rogalski, "Infrared detectors: an overview," Infrared Phys. Technol. **43**(3-5), 187–210 (2002).
2. A. Rogalski, "History of infrared detectors," Opto-Electron. Rev. **20**(3), 279–308 (2012).
3. S. Goossens, G. Navickaite, C. Monasterio, S. Gupta, J. J. Piqueras, R. Pérez, G. Burwell, T. Ivan Nikitskiy, T. Lasanta, T. Galán, E. Puma, A. Centeno, A. Pesquera, A. Zurutuza, G. Konstantatos, and F. Koppens, "Broadband image sensor array based on graphene–CMOS integration," Nat. Photonics **11**(6), 366–371 (2017).
4. E. Theocharous, R. Deshpande, A. C. Dillon, and J. Lehman, "Evaluation of a pyroelectric detector with a carbon multiwalled nanotube black coating in the infrared," Appl. Opt. **45**(6), 1093–1097 (2006).
5. L. Tang, S. E. Kocabas, S. Latif, A. K. Okyay, D. S. Ly-Gagnon, K. C. Saraswat, and D. A. B. Miller, "Nanometre-scale germanium photodetector enhanced by a near-infrared dipole antenna," Nat. Photonics **2**(4), 226–229 (2008).
6. F. Marsili, V. B. Verma, J. A. Stern, S. Harrington, A. E. Lita, T. Gerrits, I. Vayshenker, B. Baek, M. D. Shaw, R. P. Mirin, and S. W. Nam, "Detecting single infrared photons with 93% system efficiency," Nat. Photonics **7**(3), 210–214 (2013).
7. M. Wu, D. N. Congreve, M. W. B. Wilson, J. Jean, N. Geva, M. Welborn, T. Van Voorhis, V. Bulović, M. G. Bawendi, and M. A. Baldo, "Solid-state infrared-to-visible upconversion sensitized by colloidal nanocrystals," Nat. Photonics **10**(1), 31–34 (2016).
8. P. W. Kruse, *Uncooled Thermal Imaging - Arrays, Systems, and Applications* (SPIE, 2001).
9. M. T. Mueller, A. P. Pisano, R. Azevedo, D. C. Walther, D. R. Myers, and M. Wasilik, Patent No. WO 2009039193 A1 (2009).
10. A. D. Pris, Y. Utturkar, C. Surman, W. G. Morris, A. Vert, S. Zalyubovskiy, T. Deng, H. T. Ghiradella, and R. A. Potyrailo, "Towards high-speed imaging of infrared photons with bio-inspired nanoarchitectures," Nat. Photonics **6**(3), 195–200 (2012).
11. F. Zhang, Q. Shen, X. Shi, S. Li, W. Wang, Z. Luo, G. He, P. Zhang, P. Tao, C. Song, W. Zhang, D. Zhang, T. Deng, and W. Shang, "Infrared Detection Based on Localized Modification of Morpho Butterfly Wings," Adv. Mater. **27**(6), 1077–1082 (2015).
12. S. Berthier, *Photonique des Morphos* (Springer Science & Business Media, 2010).

#324687 https://doi.org/10.1364/OE.26.014143
Journal © 2018 Received 21 Feb 2018; revised 20 Apr 2018; accepted 26 Apr 2018; published 18 May 2018

13. T. Shimobaba, J. T. Weng, T. Sakurai, N. Okada, T. Nishitsuji, N. Takada, A. Shiraki, N. Masuda, and T. Ito, "Computational wave optics library for C++: CWO++ library," Comput. Phys. Commun. **183**(5), 1124–1138 (2012).
14. D. G. Stavenga, H. L. Leertouwer, T. Hariyama, H. A. De Raedt, and B. D. Wilts, "Sexual dichromatism of the damselfly Calopteryx japonica caused by a melanin-chitin multilayer in the male wing veins," PLoS One **7**(11), e49743 (2012).
15. C. L. Phillips, J. M. Parr, and E. A. Riskin, *Signals, Systems and Transforms* (Pearson Education, Inc., 2008).
16. Y. Ogawa, R. Hori, U.-J. Kim, and M. Wada, "Elastic modulus in the crystalline region and the thermal expansion coefficients of α-chitin determined using synchrotron radiated X-ray diffraction," Carbohydr. Polym. **83**(3), 1213–1217 (2011).
17. J. F. Vincent and U. G. K. Wegst, "Design and mechanical properties of insect cuticle," Arthropod Struct. Dev. **33**(3), 187–199 (2004).
18. S. G. Jennings, "The mean free path in air," J. Aerosol Sci. **19**(2), 159–166 (1988).
19. A. Ventura, N. Gimelshein, S. Gimelshein, and A. Ketsdever, "Effect of vane thickness on radiometric force," J. Fluid Mech. **735**, 684–704 (2013).
20. M. R. Cardenas, I. Graur, P. Perrier, and J. G. Meolans, "Thermal transpiration flow: A circular cross-section microtube submitted to a temperature gradient," Phys. Fluids **23**(3), 031702 (2011).
21. A. Passian, A. Wig, F. Meriaudeau, T. L. Ferrell, and T. Thundat, "Knudsen forces on microcantilevers," J. Appl. Phys. **92**(10), 6326–6333 (2002).
22. N. K. Gupta and Y. B. Gianchandani, "Thermal transpiration in zeolites: A mechanism for motionless gas pumps," Appl. Phys. Lett. **93**(19), 193511 (2008).
23. V. G. Shvedov, A. V. Rode, Y. V. Izdebskaya, A. S. Desyatnikov, W. Krolikowski, and Y. S. Kivshar, "Giant Optical Manipulation," Phys. Rev. Lett. **105**(11), 118103 (2010).
24. B. Gotsmann and U. Duerig, "Experimental observation of attractive and repolsive thermal forces on microcantilevers," Appl. Phys. Lett. **87**(19), 194102 (2005).
25. T. Kreis, *Handbook of Holographic Interferometry Optical and Digital Methods* (WILEY-VCH, 2005).
26. S. Zhang and Y. Chen, "Nanofabrication and coloration study of artificial Morpho butterfly wings with aligned lamellae layers," Sci. Rep. **5**(1), 16637 (2015).
27. M. A. Giraldo and D. G. Stavenga, "Brilliant iridescence of Morpho butterfly wing scales is due to both a thin film lower lamina and a multilayered upper lamina," J. Comp. Physiol. A Neuroethol. Sens. Neural Behav. Physiol. **202**(5), 381–388 (2016).
28. T. Kampfrath, K. von Volkmann, C. M. Aguirre, P. Desjardins, R. Martel, M. Krenz, C. Frischkorn, M. Wolf, and L. Perfetti, "Mechanism of the Far-Infrared Absorption of Carbon-Nanotube Films," Phys. Rev. Lett. **101**(26), 267403 (2008).
29. X. Xin, H. Altan, A. Sainta, D. Matten, and R. R. Alfano, "Terahertz absorption spectrum of para and ortho water vapors at different humidities at room temperature," J. Appl. Phys. **100**(9), 094905 (2006).
30. D. V. Pantelić, D. Ž. Grujić, and D. M. Vasiljević, "Single-beam, dual-view digital holographic interferometry for biomechanical strain measurements of biological objects," J. Biomed. Opt. **19**(12), 127005 (2014).
31. R. B. Hetnarski and M. R. Eslami, *Thermal Stresses - Advanced Theory and Applications* (Springer, 2009).
32. C. Y. Young and R. G. Budynas, *Roark's Formulas for Stress and Strain*, 7th ed. (McGraw-Hill, 2002).
33. O. A. Bauchau and J. I. Craig, *Structural Analysis with Applications to Aerospace Structures* (Springer, 2009).

1. Introduction

Infrared (IR) detectors are widely used nowadays with many possible applications in astronomy, medicine, military, automotive industry, and many more. They can be divided in two large groups - thermal and quantum [1] - based on the working principle. Quantum-detection sensors produce electrical output due to the direct conversion of IR signal into electric energy. They have high detection efficiency and very fast response, but cryogenic cooling is required, making them sensitive and expensive. Thermal detectors are heated as a result of absorption, altering some physical property of a material with subsequent conversion to electrical signal [2]. They are slower, but work at room temperature. New ideas abound, such as IR detection based on graphene [3], carbon nanotubes [4], quantum dots [5], superconducting nano-wires [6] or up-conversion [7]. Common to all of them is a complicated construction, complex manufacturing technologies and intricate underlying physics.

Generally, arrays of IR thermal detectors were used for imaging camera construction [8]. Based on their mode of operation and cooling requirements, thermal cameras are classified as cooled (requiring cryogenic system such as Stirling machine) and uncooled, which are much simpler and more versatile.

Optics EXPRESS

A large group of uncooled cameras are based on bi-material, micromechanical cantilevers, whose radiation-induced mechanical deformation is detected electrically or optically. To amplify the thermo-mechanical response, cantilevers are made of two materials with different thermal expansion coefficient (usually metals or semiconductors, but materials of biologic origin, such as chitin or proteins, present a viable option [9], too).

Natural biological structures can be turned into IR detectors by using thermally-induced spectral change of wing-scales iridescence [10]. It was proposed that thermal dilatation of wing scales increases the distance between the Brag-grating-like lamellas and changes the refractive index, thus inducing a slight shift of the iridescence spectrum. Due to low thermal expansion coefficient (50×10^{-6} K^{-1}) the final effect is very small and differential spectrometry is used for detection. The thermal response was further improved by coating wing scales with carbon nanotubes. In another line of research [11], wing scales were covered with a thin layer of gold in order to produce bi-material structure which bends upon heating. In both cases, the detection principle renders spatially resolved imaging very difficult, and strongly limited by the thermal expansion coefficient, leaving little room for further improvements.

Here we present an infrared imaging system with *Morpho menelaus* butterfly wing as a sensing medium. Digital holographic interferometry was used to detect thermally-induced displacements. The spatial resolution is of the order of the butterfly wing-scale (approximately 50 × 100 μm [12]), the temperature sensitivity is 2.8 mK and the response frequency around 200 Hz, which is quite comparable to high level commercial cameras. Sensitivity is much higher than could have been expected from the thermal dilatation coefficient alone and we propose that photophoretic forces are responsible for the effect. We have calculated the photophoretic pressure and the resulting displacements of butterfly scales, finding them in good agreement with the experimental results.

2. Infrared imaging on a butterfly's wing

The detection of infrared radiation was done using a *Morpho menelaus* butterfly wing, whose circular section, 1 cm diameter, was extracted from a wing, putting some effort to choose a zone devoid of wing-veins as much as possible. Section was attached to the holder with a double adhesive tape, without any special preparations, see Fig. 1(a). As can be seen in Fig. 1(b), the wing is densely covered with iridescent particles shaped as micro-cantilevers possessing nanoscale, layered structures, see inset of a Fig. 1(b). The wing-section was irradiated with near IR laser beam for localized heating of the wing. A thermal process was monitored holographically, using a setup and method described in a Section A.1 of the Appendix. We were able to reconstruct a single diffraction order of a hologram at 2048 × 2048 resolution due to properties of the shifted Fresnel transform [13]. All the details of the wing were clearly revealed, as shown in Fig. 1(c). By producing an interferogram between the reference hologram (recorded before switching-on the 980 nm laser) and the one recorded during the thermal process, we were able to faithfully observe the elongated laser beam shape, as shown in Fig. 1(d).

The laser beam power was kept constant and the pulse duration was decreased until no beam trace was discernible by the holographic interferometry. In this way the detection threshold was established at several μJ/cm^2, depending on the wavelength. This is because we used a butterfly wing as it is, without further functionalization or alteration and the temperature increase is determined by its natural absorptivity. It is well known that the melanin is a constituent of wing scales, with absorptivity being much higher at UV than in IR [14], thus explaining the lower detection threshold in UV.

We used commercial thermal camera (FLIR SC620, 640 × 480 pixel, 40 mK thermal resolution, and maximum speed of 120 fps at reduced resolution) to establish the relation between the temperature of the wing and holographically measured phase difference (see section A.1 of the Appendix for details).

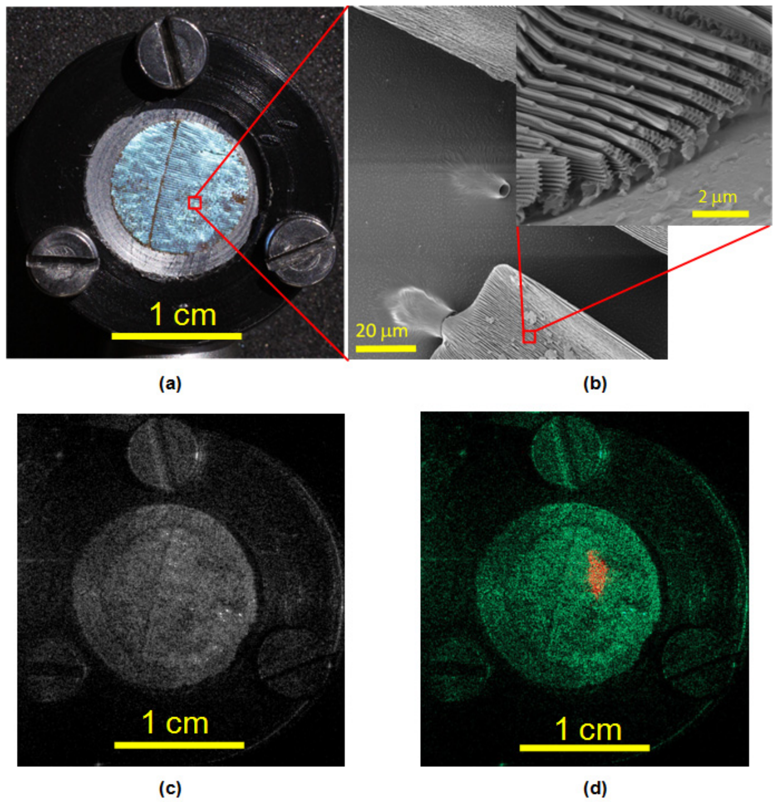

Fig. 1. (a) A photograph of a circular section of a *Morpho menelaus* butterfly wing attached to a holder. (b) SEM image showing the cantilever-like structure of the *Morpho menelaus* wing-scale and (see inset) ultrastructure of its surface, with a number of lamellae. (c) A hologram reconstruction of a section of the butterfly wing. (d) A holographic image obtained after irradiation of a butterfly wing with a 980 nm pulsed laser beam (having elliptical beam profile 2.7 mm × 6.8 mm, 8.7 mW power and 128 ms pulse length, corresponding to ~2 mJ/cm^2 energy density).

Thus, the same thermal process was monitored by the thermal camera [depicted in Figs. 2(a) and 2(b)] and our method [Fig. 2(c)]. We have found that the temperature rise of ΔT = 0.4 K, recorded by the IR camera corresponds to holographically detected phase difference $\Delta\Phi$ = 5.1 rad, i.e. to the displacement of 0.432 µm. The related thermo-mechanical response is, therefore, 1.08 µm/K. Based on that and experimentally recorded phase-noise level (Φ_n = 0.037 rad, corresponding to resolvable displacement of the order of 3.1 nm), we found the temperature detection sensitivity of 2.9 mK.

According to the theory of linear time-invariant systems [15], impulse response can be determined by differentiating its Heaviside step response, and a transfer function is further found by Fourier transforming the impulse response. Thermal systems can be treated as linear, because conductive, convective and radiation thermal energy exchange can be modeled by the linear differential equations. That is why the thermal response of the wing was determined by irradiation with a long laser pulse (at 980 nm and 8.7 mW). The response was Fourier transformed to obtain the transfer function, displayed in Fig. 3. For a 10 dB signal-to-noise ratio (SNR) the detection frequency is 30 Hz, while for 20 dB SNR detection frequency is larger than 200 Hz, see Fig. 3.

Optics EXPRESS

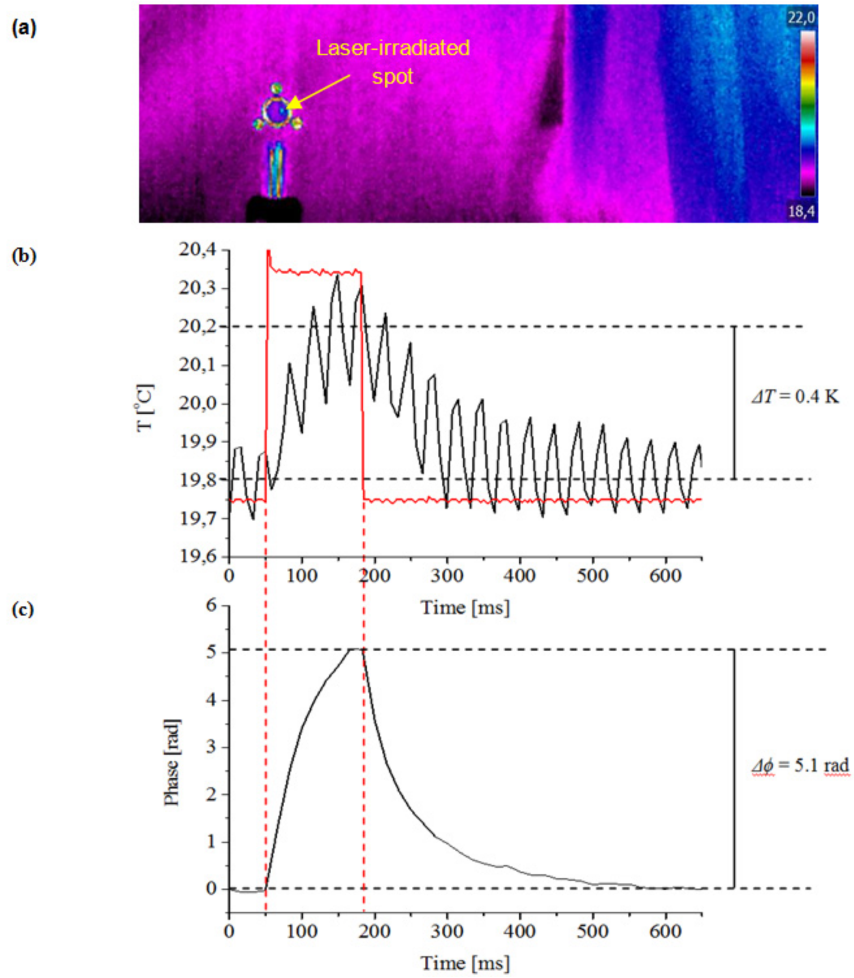

Fig. 2. (a) Thermal camera image of the butterfly wing section irradiated with the laser beam (at 980 nm wavelength, 8.7 mW power and 128 ms pulse length). (b) Temperature variation (black line) recorded by the thermal camera during laser irradiation. Fast oscillations are camera noise. A laser pulse shape (red line) is shown, too. (c) A corresponding phase difference recorded holographically under the same conditions.

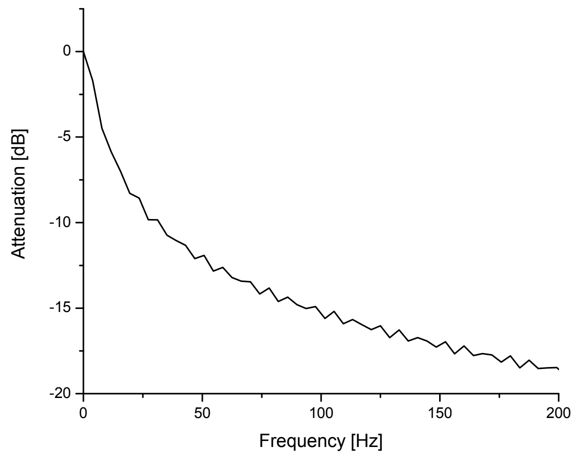

Fig. 3. Attenuation of the butterfly's wing response as a function of signal frequency.

3. Thermo-mechanics of the wing-scales

Radiation-induced temperature rise produces a thermal dilatation and bending of wing-scales, which were calculated at 0.005 μm/K and 0.029 μm/K, respectively (see Section A.2 of the Appendix for a detailed analysis). This is more than an order of magnitude lower than experimentally observed 1.08 μm/K. To resolve the discrepancy, we were motivated to take a closer look at the morphological, absorptive, thermal and mechanical properties of the *Morpho menelaus* wing-scales.

Each scale is almost a flat plate (approximately 100 μm long, 50 μm wide and 2 μm thick [12]) embedded in the wing membrane by its pedicle [Fig. 1(b)] and acting just like a mechanical cantilever. The scale's main, plate-like, body has two laminae: the lower one being almost flat, while the upper is structured with densely packed ridges, made of a number of lamellas [10], see inset in Fig. 1(b). As of the material properties (mostly chitin), a thermal expansion coefficient is $k = 50 \times 10^{-6}$ K^{-1} [10, 16], modulus of elasticity E is estimated between 2 GPa and 20 GPa [17] and we measured the absorption coefficient of the wing $\alpha = 4.5 \times 10^{-4}$ nm^{-1} at 980 nm.

Here we claim that the additional mechanical force comes from molecular interaction between the surrounding gas and the heated nanostructures of the wing-scales The mean free path of molecules in air is generally accepted to be around 66 nm at the ambient pressure (~10^5 Pa) [18], according to kinetic theory of gasses. This is quite comparable to the lamellar spacing of the wing-scale (150 nm). Under such circumstances, the inter-lamellar space is so small that only a few hundred atoms fit in-between, see Fig. 4. Numerically, the situation is described by the Knudsen number K_n, defined as a ratio between the mean free path of the surrounding fluid and the characteristic dimension of the system (in our case, the distance between lamellas). If a thermal gradient is established in a thermodynamic system with the Knudsen number between 0.1 and 10, an additional, so-called radiometric (Knudsen) forces appear [19]. This is exactly the situation of a radiatively-heated wing-scale, where the temperature difference is established and the Knudsen number is 0.45.

The radiometric forces have been investigated in many different circumstances connected with thermal transpiration [20], AFM cantilevers in partial vacuum [21] or pumps without moving parts [22]. The same effect has been used to mechanically manipulate large particles using vortex or bottle beams [23].

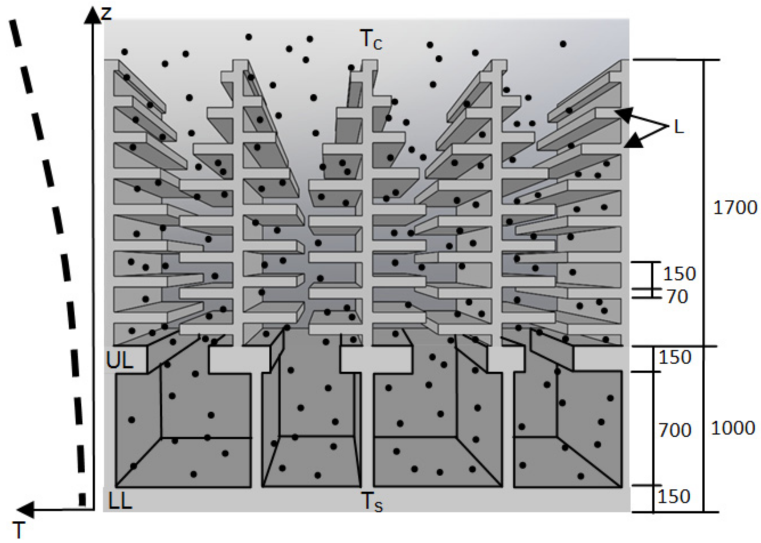

Fig. 4. Scheme of the cross-section of a *Morpho* butterfly scale. Black dots represent molecules of air at atmospheric conditions. A radiation-induced temperature gradient (black dashed line) is established across the wing scale (T_s<T_c). Dimensions are in nanometers but the drawing is not to the scale. L – lamellae, UL – upper lamina, LL – lower lamina.

We have studied the effects of radiometric forces using a theory developed by Passian [21], which was slightly amended and experimentally tested in [24]. For ambient conditions corresponding to our experiments (normal atmospheric pressure 10^5 Pa and room temperature 295 K) and the temperature gradient of 0.31 K (corresponding to temperature increase of 1 K) we have calculated that the resulting photophoretic pressure is 26.3 Pa (see Section A.3.1 of the Appendix for details).

In order to estimate the associated mechanical deformation, we use a simplified mechanical model of a butterfly wing-scale, shown schematically in Fig. 5(a). This is a combination of a thin, corrugated, hollow box (imitating the main body - flattened part - of the scale) attached to a short beam, rigidly constrained at its end (approximating the scale pedicle). An approximate analytic solution for the maximum displacement of the mechanical model was found, showing the influence of mechanical parameters of the system on thermo-mechanical response (see Section A.3.2 of the Appendix). More accurate solution was found using finite element method (FEM) based on the model shown in Fig. 5(b). The corresponding displacement field was calculated and shown in Fig. 5(c), based on mechanical parameters given in Table 1. of the A.3.2 Appendix section.

By taking dimensional parameters of the wing-scales from [10,12] [which closely correspond to our SEM images – see inset in Fig. 1(b)], photophporetic pressure calculated above and modulus of elasticity of 18 GPa, taken from the available literature [17], we found that scale-tip displacement is 1.16 μm/K, in agreement with experimentally obtained value.

Optics EXPRESS

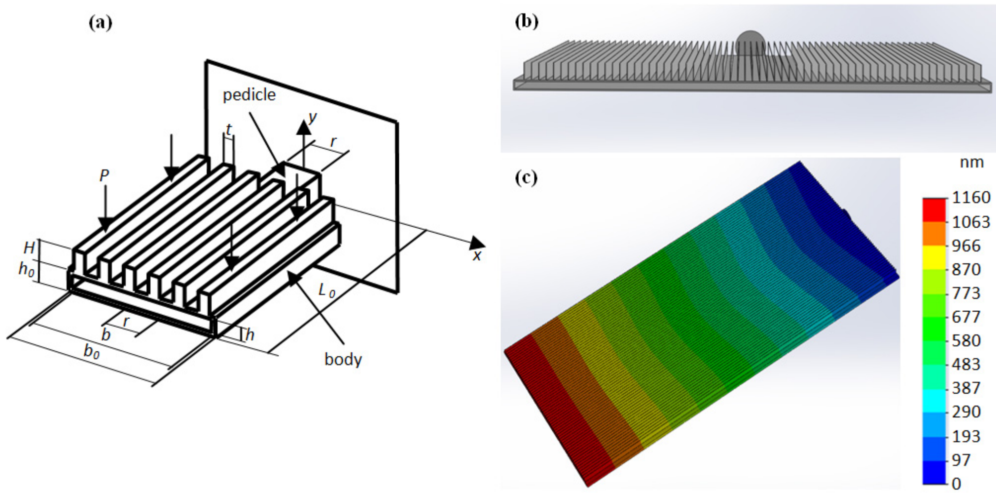

Fig. 5. (a) Scheme of the butterfly wing-scale with dimensional parameters. (b) Perspective view of the FEM wing-scale model. (c) Perspective view of the butterfly wing-scale deflection field.

4. Discussion

We used holography for detection, because imaging is very sensitive, straightforward and easy to implement. We found that the classical problems of mechanical stability, ambient conditions like air currents, vibration, and acoustic disturbances, were completely unimportant in our single-beam setup, described earlier and in the Appendix. Heating of the butterfly wing by the holographic reference beam itself is unimportant because it is constant, of low intensity (110 µW/cm2 at 532 nm) and makes uniform background which cancels in interferometric measurements. However, intensity stability of the beam must be such that the induced temperature variations are below the detection threshold, which was satisfied in our experiments (laser stability 1.28%, RMS noise 0.17%, according to manufacturer). The angle between the reference beam and observation direction is small and the holographic sensitivity (influenced by the sensitivity vector [25]) is close to 1. This means that the one fringe displacement is very close to the wavelength (532 nm in our case). For larger photophoretic displacements, we have observed phase wrapping, which was easily corrected (by phase un-wrapping [25]).

Butterfly wings are not an ideal imaging detector. Wing-scales are not distributed evenly, their shape, position, anatomy and mechanical properties are not uniform, some zones are depleted [such as wing veins – as can be seen in Fig. 1(a)] and the wing surface is wavy. As a result, different wing zones and wing scales produce variable response. This is a well known problem in thermal camera construction, corrected by, so called, non-uniformity compensation. Here we made no attempt to improve the situation because the proper equipment was not available to us. For the same reason, we were also unable to measure the noise equivalent thermal difference (NETD), because it includes an infrared imaging system and a low temperature black body. All measurements in our work express the value of thermal sensitivity of the butterfly wing, used as a focal point array.

Anyway, we think that significant improvements can be made to the photophoretically active surface. Quite large wing portions with better uniformity can be selected (especially on *Morpho* butterflies), cut and tiled to make a larger detection surface. In that respect, we have demonstrated that butterfly wings can be precisely cut and scribed by a femto-second laser. It could be expected that the photophoretic effect largely depends on the butterfly species and will be maximized for insects with intricate nanostructures (day flying butterflies, e.g. lycaenidae, nymphalidae). Alternatively, wing scales can be harvested, manipulated and attached to an artificial substrate in an orderly manner. Finally, photophoretic principle can be used in a completely artificial system imitating to some degree wing scales - see structures described in [26].

The spatial resolution of the described butterfly-wing-based sensor is determined by the length of the scales, because the maximum deflection is at the tip. For regions closer to the petal deflection is much lower and drops below the detection capabilities of holographic interferometry. We found that the resolving power of the holographic setup is 19.5 µm x 29.5 µm, according to Rayleigh criterion. This was defined by the detector chip size (13.2 × 8.8 mm) and its distance to the butterfly wing (800 mm). The resolution can be significantly improved by reducing the distance in a holographic setup and by using a larger detector chip size.

There is also an important question of efficient absorption of electro-magnetic radiation by the wing scales. We used completely unmodified wing with naturally present, chitin, pigments and proteins. Presence of melanin is well established in Morpho wing scales [27] resulting in much higher absorption in the blue-UV, compared to IR spectral range. We really observed that the detection sensitivity at 405 nm is much higher than at 980 nm. We used a Fourier-transform infrared (FTIR) spectrometer to measure the far infrared spectrum of the Morpho wing, where we found two prospective regions (2800-3300 nm and 5700-6600 nm) with absorption as high as 50%. With proper sensitization (e.g. single-walled carbon nanotubes or water), detection of far IR [28] and terahertz radiation is possible [29], too. Therefore, these nature-based structures can be modified into a thermal detector sensitive within an extremely wide spectral range of electro-magnetic radiation.

With regard to photophoresis, we see additional possibilities to amplify the effect by changing the chemical composition of the gas and its pressure or increase the temperature and thermal gradient, by proper sensitization of the base material. So far, photophoresis was studied in simple systems like AFM cantilevers [21] or spherical particles [23], and adequate models should be developed for butterfly-like structures, with a number of Bragg layers or photonic crystals.

We emphasize that the radiation detection, within the IR power range used in this research, is completely nondestructive to the wing. We used the same wing for months without any deterioration or damage. The fact is supported by hundred years old butterfly specimens in entomological collections, still retaining their structural color.

It should be added that the principle of electrophoretic radiation detection is universal and applicable to other types of invisible radiation (UV, terahertz). There are a number of things that can be optimized to improve the sensitivity and spatial resolution of the system, such as: building an artificial micro-cantilever array, changing dimensions and material composition of micro-cantilevers, adjusting chemical composition of gaseous environment, designing other, nonoptical, readout methods (e.g. capacitive, piezo or resistive). Findings of this experiment and results of the model can be an inspiration for fabrication of butterfly-inspired thermal chip. For example, by using elastomeric cantilever made of PDMS, whose modulus of elasticity is three orders of magnitude lower compared to wing-scales used in this research, we can expect three orders of magnitude larger thermal sensitivity. Even the existing systems based on bi-material cantilevers could be improved by nano-patterning to introduce additional photophoretic effect.

5. Conclusion

A novel method of detecting low level thermal radiation, using scales of the *Morpho menelaus* butterfly wing, is presented. Thermally induced displacements of scales were measured using digital holography. We have found that characteristics of this, nature-given sensing elements are quite promising, even when compared with the state-of-the-art thermal cameras. Temperature detection sensitivity is 2.9 mK, with the detection threshold of several µJ/cm^2, depending on the wavelength. The detection frequency reaches over 200 Hz, for SNR of 20 dB. We emphasized a strong mechanical stability and durability of butterfly wings, and completely nondestructive nature of measurements.

We have found that the photophoresis at atmospheric pressure is the underlying mechanism, as verified by measurements and a simplified mechanical model of the wing-scale. The resulting, photophoretically induced, displacement was 1.16 μm/K, in agreement with the experiment.

The described method of thermal radiation detection is universally applicable and will function with other manmade materials and structures, as long as the characteristic size of structures is comparable to the mean free path of molecules of the surrounding gas.

Appendix

A.1 Holographic setup and phase measurements

A simple setup described previously [30] and shown in Fig. 6. was used throughout this research. A beam from the unmodulated laser L1 (Torus 532 laser, manufactured by Laser Quantum, with 532 nm wavelength, 43.1 mW power and 10 m coherence length) is spatially filtered by focusing the laser beam (with a biconvex lens L with 50 mm focal length) through the 25 μm diameter pinhole P. The resulting laser beam is directed towards the concave mirror CM with 75.3 mm aperture diameter and 23 mm focal length. Part of the divergent laser beam directly illuminates the wing section W mounted in front of the concave mirror CM, thus generating an object beam O. The rest of the beam, which misses the object W, generates the reference beam R. A mirrorless CMOS camera C (Nikon 1v3, detector size 13.2 × 8.8 mm, 18.4 MPixel, 60 frames per second) is placed in a zone where the reference beam R interferes with the object beam O, scattered from the wing section W. Laser L2 at 980 nm (with elliptical, divergent beam and 30 mW maximum power) was used, as a source of NIR radiation, to irradiate the butterfly wing section W. Its power was adjusted by a variable beam-attenuator, and irradiation time was controlled by switching laser on and off, using Arduino Mega 2560 Rev3 microcontroller. Laser (L2) produced thermal fingerprint on the butterfly wing which was detected holographically. The setup is mechanically extremely stable and we needed no vibration isolation.

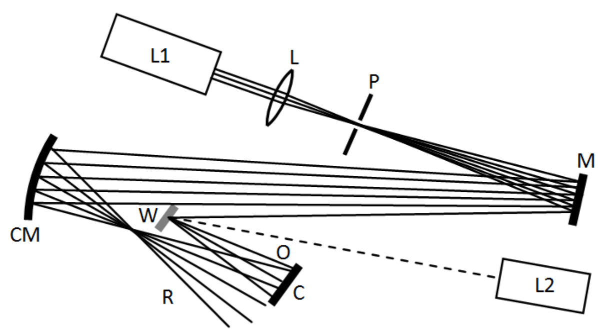

Fig. 6. Scheme of a holographic device used to detect photophoretic displacement of a butterfly's wing. L1 – laser at 532 nm, L2 - laser at 980 nm, L – biconvex lens, CM – concave mirror, C – CMOS camera, W – butterfly wing section, R – reference beam, O – object beam, P – a pinhole used for spatial filtering of the laser beam, M – a flat mirror used to deflect the laser beam.

Holographic measurements were performed as follows. A camera C was turned-on for approximately 50 ms (corresponding to about 3 frames) before the infrared laser L2 was turned-on for 128 ms. Recording was continued even after turning the laser off, in order to monitor the wing cooling process. Total number of holograms was 40, during the recording time of 670 ms. Holograms were then numerically reconstructed using shifted Fresnel transform algorithm, implemented on a CUDA-enabled graphics card (ASUS Expedition

GeForce GTX 1050 Ti) [13]. As a result, a time series of butterfly wing images was produced, containing both amplitude [see Fig. 1(c)] and phase information. Phase values of the first reconstructed image were taken as a reference. A phase difference between the reference and subsequent images were calculated and depicted in Fig. 2(c).

A.2 Thermal gradient across the butterfly's scale

Radiation is partially absorbed by the wing scales leading to the temperature increase. Here we establish a connection between the average temperature increase of the wing scale (which is measurable) and the thermal gradient across the scale (which is not measurable, due to smallness of the scale). A butterfly wing scale will be approximated by a number of layers having certain thicknesses D_j, masses M_j, and absorptivities A_j, as depicted in Fig. 7(a).

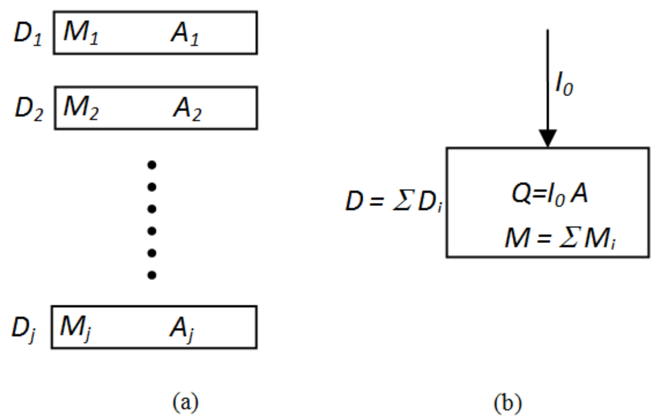

Fig. 7. (a) Layers of the wing scale with their masses M_j, thicknesses D_j and absorptivities A_j. (b) A single wing scale treated as a bulk body having the mass M and thickness D equal to sum of masses and thicknesses of its layers. I_0 is radiation intensity, A is absorptivity, and Q absorbed energy.

First we will treat the scale as a monolithic body [Fig. 7(b)] having thickness D and mass M equal to the sum of thicknesses D_j and masses M_j of its individual layers. Suppose that the incident light has intensity I_0, and that the fraction A of the incident energy is absorbed by the scale, i.e. energy $Q = I_0A$ is dissipated in the scale. This energy is used to increase the temperature (by amount ΔT) of the scale having total mass M and specific heat c. A temperature increase ΔT is actually an average temperature of the wing-scale (the only measurable parameter, due to the thinness of the scale). The process is described by:

$$Q = Mc\Delta T, \tag{1}$$

$$I_0 A = Mc\Delta T, \tag{2}$$

$$I_0 = \frac{Mc\Delta T}{A}. \tag{3}$$

We are now going to treat a scale as layered structure, as can be seen in the Fig. 7(b). A fraction A_j of the input energy I_0 is absorbed by the layer j, i.e. $Q_j = I_0A_j$ and the temperature will increase by ΔT_j as:

$$I_0 A_j = M_j c\Delta T_j. \tag{4}$$

By introducing Eq. (3) into Eq. (4), we get:

$$\Delta T_j = \frac{M}{M_j}\frac{A_j}{A}\Delta T. \tag{5}$$

Optics EXPRESS

Let's analyze the temperature rise of the *j*-th layer having volume $\Delta V_j = \Delta x \Delta y D_j$ (where D_j, Δx, Δy and ρ are thicknesses, width, length and density, respectively). Taking into account that $M_j = \rho \Delta V_j = \rho \Delta x \Delta y D_j$ and using Eq. (5) we then get:

$$\Delta T_j = \frac{\sum_{j=1} M_j}{M_j} \frac{A_j}{A} \Delta T = \frac{\sum_{j=1} D_j}{D_j} \frac{A_j}{A} \Delta T = \frac{D}{D_j} \frac{A_j}{A} \Delta T. \tag{6}$$

From measured absorptivity of the *Morpho* wing at 980 nm we calculated the coefficient of absorption as $\alpha = 4.5 \times 10^{-4}$. Fractions of absorbed energy A and A_j were calculated using Lambert-Beer's law [$I = I_0 exp(-\alpha D)$]. We are now able to calculate the temperature distribution across the wing scale, assuming 7 lamelae, having equal thickness of 70 nm, and two laminae with 150 nm thickness, each. If the average increase of temperature is $\Delta T = 1$ K, we get the temperature distribution depicted in Fig. 8. As can be seen, the average temperature increase is 1 K, but the temperature difference across the scale is $\delta_T = 0.31$ K.

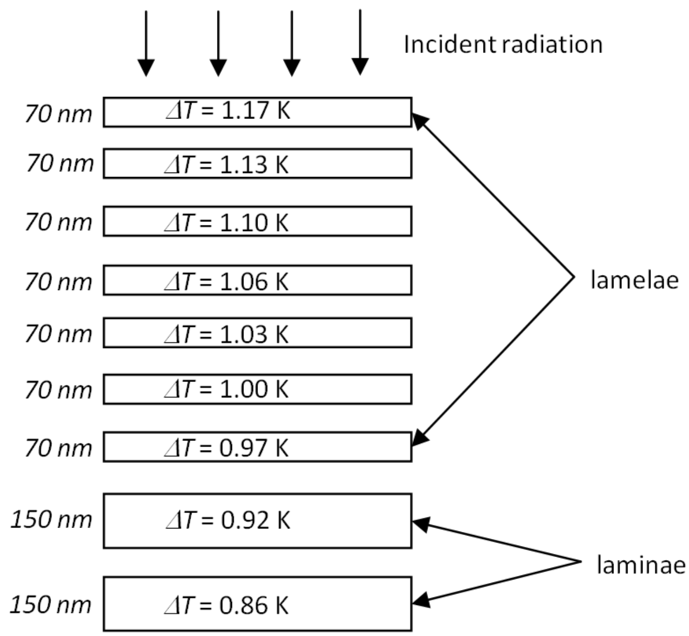

Fig. 8. Temperature gradient along the wing-scale having the average temperature increase of 1K, assuming the coefficient of absorption $\alpha = 4.5 \cdot 10^{-4}$.

This motivated us to treat the wing-scale as a nonuniformly heated cantilever, which bends as a result of uneven dilatation. This is a well known problem in mechanics and the maximum deflection Δ_0 of the cantilever tip is given by the following equation (see chapter 5 in [31]):

$$\Delta_0 = \frac{k L_0^2}{2} \frac{\delta_T}{t}, \tag{7}$$

where k is a coefficient of thermal expansion, L_0 is a cantilever length, t is its thickness and δ_T is a temperature difference established between cantilever's top and bottom surfaces. We found that, for $\delta_T = 0.31$ K, total thickness of the scale of $t = 2.7$ µm, length $L_0 = 100$ µm and $k = 5 \cdot 10^{-5}$ 1/K the corresponding maximum deflection is 0.029 µm/K [using Eq. (7)]. This is still much lower than, holographically observed, 1.08µm/K.

Optics EXPRESS

A.3 Calculation of mechanical effects due to photophoretic pressure

A.3.1 Photophoretic pressure

A fluid inside the wing scale cannot be treated as continuum, but as free molecules where molecule-surface (of the scale lamellae) collisions dominate molecule-molecule collisions. A simplified model [schematically shown in Fig. 9] was developed in [21,21], where the thermodynamic system consists of a substrate S at temperature T_s, thin membrane M at temperature T_c, embedded in a fluid with temperature T_r, and the distance between the substrate and membrane is of the order of the mean path length of the fluid. It was found that the resulting radiometric pressure P is described by the following expression [21,24]:

$$P = \frac{P_r}{2}\left[\begin{array}{l}\sqrt{\frac{a_s\tau_s + a_{cb}\left(1-a_s\right)\tau_c}{a_s + a_{cb} - a_s a_{cb}}} + \\ \sqrt{\frac{a_{cb}\tau_c + a_s\left(1-a_{cb}\right)\tau_s}{a_s + a_{cb} - a_s a_{cb}}} \\ -\sqrt{1-a_{ct}+a_{ct}\tau_c} - 1\end{array}\right], \tag{8}$$

where P_r is environmental pressure, a_s, a_{ct}, a_{cb} are accommodation coefficients of the substrate and membrane surfaces [Fig. 9], and $\tau_c = T_c/T_r$, $\tau_s = T_s/T_r$ are relative temperatures (relative to ambient temperature T_r).

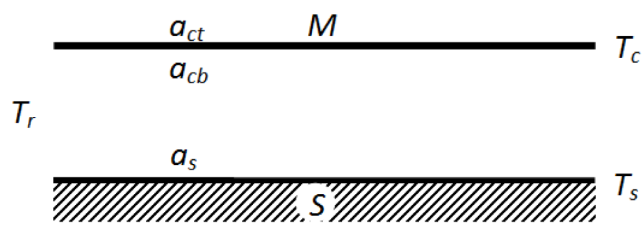

Fig. 9. A scheme of a radiometric system embedded in a fluid with temperature T_r, having a substrate S at temperature T_s, thin membrane M at temperature T_c, surfaces having accommodation coefficients a_s, a_{ct}, a_{cb}, and the spacing between the substrate and membrane is of the order of the mean free path of the gas molecules.

For the purpose of this study we will slightly modify the Eq. (8), by assuming that all surfaces are identical and diffusely reflect molecules. In that case accommodation coefficients are all equal to 1 (diffuse scattering) $a_s= a_{ct}= a_{cb}=1$. Also, assuming that the substrate S temperature is slightly above the ambient $T_s=T_r+\delta_T$, and the Eq. (8) reduces to:

$$\begin{aligned} P &= \frac{P_r}{2}\left[\sqrt{\tau_s} - 1\right] \\ &= \frac{P_r}{2}\left[\sqrt{\frac{T_r+\delta_T}{T_r}} - 1\right] \\ &= \frac{P_r}{2}\left[\sqrt{1+\frac{\delta_T}{T_r}} - 1\right]. \end{aligned} \tag{9}$$

If the temperature increase δ_T is small, compared to the ambient temperature, square root can be approximated by the first two members of a Taylor series, producing the simple equation for the photophoretic pressure:

$$P = \frac{P_r}{2}\left[\sqrt{1+\frac{\delta_T}{T_r}}-1\right] \approx \frac{P_r}{2}\left[1+\frac{1}{2}\frac{\delta_T}{T_r}-1\right] = \frac{P_r\delta_T}{4T_r}. \tag{10}$$

A.3.2 Photophoretic bending of the wing-scale

From the mechanical point of view, a butterfly wing-scale is a thin, hollow, corrugated plate attached to a short cantilever beam, see Fig. 10(a). We will treat it as a classical, simple cantilever beam [shaded gray on the Fig. 10(a)], with additional load on its left and right sides. In this way, we have a cantilever beam as in Fig. 10(b) loaded with the total force acting on the whole wing-scale body. Therefore, the resulting pressure P on the cantilever is increased by the amount equal to the ratio of the wing scale area and the beam area (equal to b_0/r), thus:

$$P = \frac{P_0 b_0}{r}. \tag{11}$$

In this way, we are left with the well-known and solved problem in mechanics [32] (within Euler-Bernoulli beam theory [33]). A maximum deflection Δ of such beam is defined as:

$$\Delta = \frac{WL_0^4}{8EI}, \tag{12}$$

where W is the load per unit length, L_0 is cantilever plate length, I is it's the second moment of cantilever cross-section and E is the modulus of elasticity. It is easy to find load per unit length as:

$$W = Pb_0. \tag{13}$$

By introducing Eqs. (10), (11) and (13) into Eq. (12) we get the final expression for the maximum deflection of the plate:

$$\Delta = \frac{1}{32E}\frac{P_r}{T_r}\frac{b_0^2 L_0^4}{rI}\delta_T. \tag{14}$$

The second moment I of the wing scale cross-section (with respect to area centroid) was calculated referring to the Fig. 10. Parameters of the theoretical model are presented in Table 1. Results of analytical expression (14) show good agreement with the FEM model [Fig. 11].

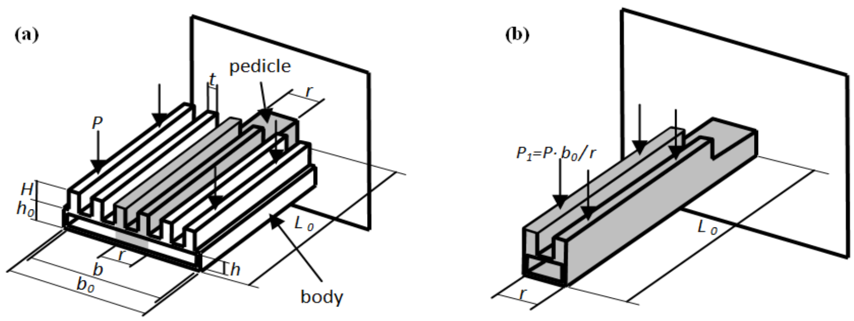

Fig. 10. (a) Butterfly wing-scale is approximated with a thin, hollow, corrugated plate attached to the short cantilever beam. (b) Approximation of a wing-scale as a beam with increased pressure due to additional force imposed by the whole scale body.

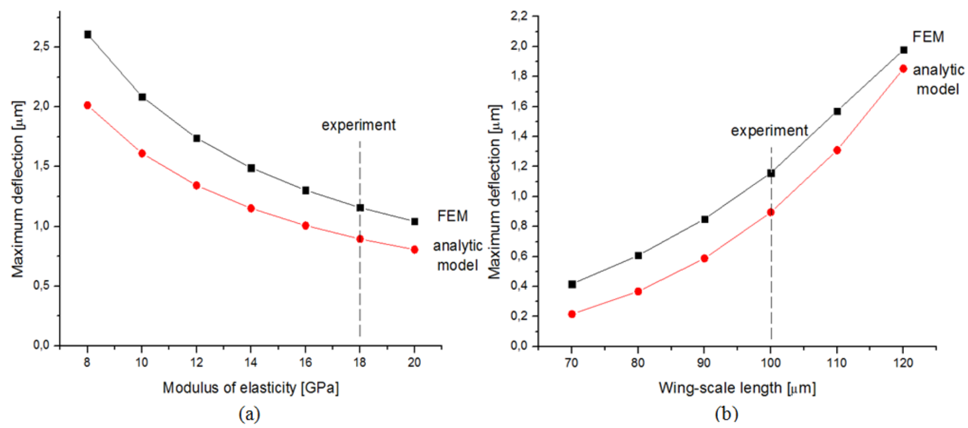

Fig. 11. Comparison between analytic and finite element methods applied to the problem of photophoretic deflection of the butterfly wing-scale. (a) Maximum deflection as a function of modulus of elasticity. (b) Maximum deflection as a function of the wing-scale length.

The second moment I of the wing scale cross-section (with respect to area centroid) was calculated referring to the Fig. 10. Parameters of the theoretical model are presented in Table 1. Results of analytical expression (14) show good agreement with the FEM model, see. Fig. 11.

Table 1. Environmental, dimensional and mechanical parameters of the butterfly wing-scale model.

environmental pressure	P_r	10^5	Pa
environmental temperature	T_r	295	K
wing-scale length	L_0	100	μm
wing-scale outer width	b_0	50	μm
wing-scale inner width	b	49.7	μm
wing-scale outer thickness	h_0	1	μm
wing-scale inner thickness	h	0.7	μm
wing-scale pedicle outer diameter	r	4	μm
wing-scale pedicle length	L	0.2	μm
ridge height	H	1.7	μm
ridge width	t	0.062	μm
modulus of elasticity	E	$18\cdot10^9$	Pa
coefficient of thermal expansion	k	$5\cdot10^{-5}$	1/K

Funding

Serbian Ministry of Education, Science and Technological Development (III45016, ON171038).

Acknowledgment

This work is done in partial fulfillment of the requirements for the PhD degree of Dusan Grujić at the University of Belgrade, Faculty of Physics.

Author contributions: D.P. conceived the idea, D.P. and D.G. constructed the holographic device and wrote the software, D.G. performed holographic measurements, D.V. and Lj.T. performed thermal camera measurements, D.V. and Z. S. modeled mechanical structure, B.J. supervised the research. D.P., D.G., B.J. and D.V. prepared the manuscript.

Opt Quant Electron (2016) 48:289
DOI 10.1007/s11082-016-0560-8

Localization of light in a polysaccharide-based complex nanostructure

Svetlana Savić-Šević[1] · Dejan Pantelić[1] · Dušan Grujić[1] · Branislav Jelenković[1]

Received: 6 November 2015 / Accepted: 7 April 2016 / Published online: 19 April 2016

Abstract An experimentally study of the coherent light scattering from disordered photonic structure is presented. We have measured the light localization length for a complex disordered multilayer system, which we have prepared by holography. The structure consisting of pullulan nanoparticles arranged in a random manner and confined between Bragg layers. The width of backscattering cone indicates a weak localization regime.

Keywords Weak localization · Backscattered cone · Photonic multilayer structure · Disorder · Polysaccharide

1 Introduction

During the past few decades, localization of light has great interest because of their applications, such as in light transport (Wiersma et al. 1997; Wiersma 2013), random lasers (Liu et al. 2014) and solar energy (Pratesi et al. 2013). Transport of light through a disordered medium can be localized by interference and multiple scattering from random structures, halting its propagation. Under the Ioffe-Regel criterion (John 1984), localization is either weak, known as coherent backscattering (when $l \sim \lambda$), or strong—Anderson localization (for $kl \leq 1$), where λ denotes laser wavelength, l is the mean free path and k is

This article is part of the Topical Collection on Advances in the Science of Light.

Guest Edited by Jelena Radovanovic, Milutin Stepic, Mikhail Sumetsky, Mauro Pereira and Dragan Indjin.

✉ Svetlana Savić-Šević
savic@ipb.ac.rs

[1] Institute of Physics, University of Belgrade, Pregrevica 118, Zemun, Belgrade 11080, Serbia

the wave number. Weak localization is a precursor to Anderson localization (Segev et al. 2013) where transport of light is a complete halt.

Coherent backscattering has been observed experimentally and studied in powders of gallium arsenide (Wiersma et al. 1997), aqueous suspensions of polystyrene particles (Wolf and Maret 1985; van Albada and Lagendijk 1985), liquid crystals (Strangi et al. 2006), animals (Jordan et al. 2014), cold atoms (Jendrzejewski et al. 2012) and in many other materials.

In this paper we have investigated backscattering of light in periodically ordered and disordered structure. We have measured the backscattered cone of light from He–Ne laser by polysaccharide-based complex nanostructure, generated by combining holography and non solvent phase separation (Li and Han 2011). Photonic structure consists of periodic ordered solid multilayer with alternately periodic multilayer of random arranged sphere, i.e. of Bragg layers filled with polydisperse nanoparticles arranged in a random way. To the best of our knowledge, results of back scattering measurements of complex structure proposed in this paper have not been published before.

2 Fabrication of photonic structures

Polysaccharide, pullulan, sensitized with ammonium dichromate (DCP-dihromated pullulan) was used as recording material (Pantelić et al. 1998; Savić et al. 2002; Savic-Ševic and Pantelic 2007). Pullulan is linear homo-polysacharide that is produced by micro-organisms of the *Aureobasidium pullulans* type (*Pullularia pullulans*) (Prajapati et al. 2013).

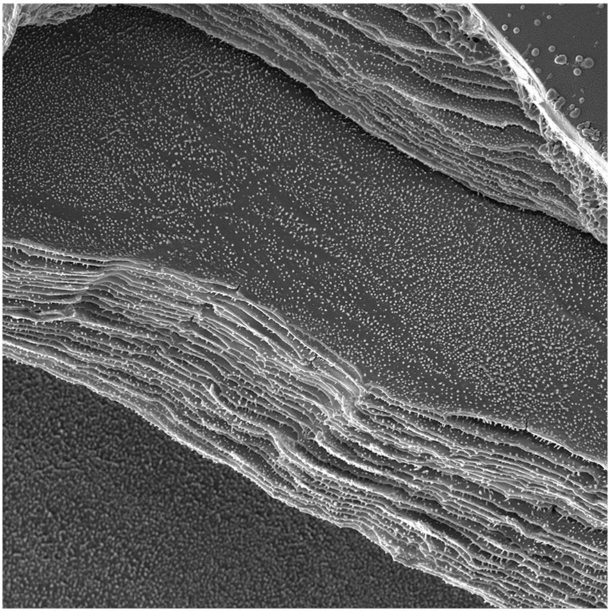

Fig. 1 FEGSEM image of internal structure of DCP grating

Photonic structures were fabricated as a volume Bragg reflection grating using a simple counter-propagating beam configuration. DCP was exposed with a single longitudinal mode, diode pumped Nd-YAG laser, at 532 nm. After exposure, grating was chemically processed in a developer. The resulting Bragg layers, upon phase separation, is filled with polydisperse, almost spherical nanoparticles arranged in a random way.

The morphology of the resulting photonic structure was investigated using a high resolution scanning electron microscope equipped with a high brightness Schottky Field Emission gun (FEGSEM). Internal structure of the DCP sample, with a number of regularly spaced Bragg layers (200 nm periods), is shown in Fig. 1. It could be seen that the Bragg grating is filled with polydisperse, almost spherical nanoparticles, with average diameter of 60 nm, arranged in a random way. Nanoparticles of pullulan are formed during phase separation.

3 Weak localization of light

Coherent light which is incident on random media is multiply elastic scattered, before exit in random direction, causing constructive interference of waves traveling in opposite directions, Fig. 2a. These randomly distributed rays interfere with each other results in enhancement of the reflected intensity (coherent back scattering) within a narrow cone with angular width (van der Mark et al. 1988),

$$W \simeq \frac{0.7\lambda}{2\pi l} \quad (1)$$

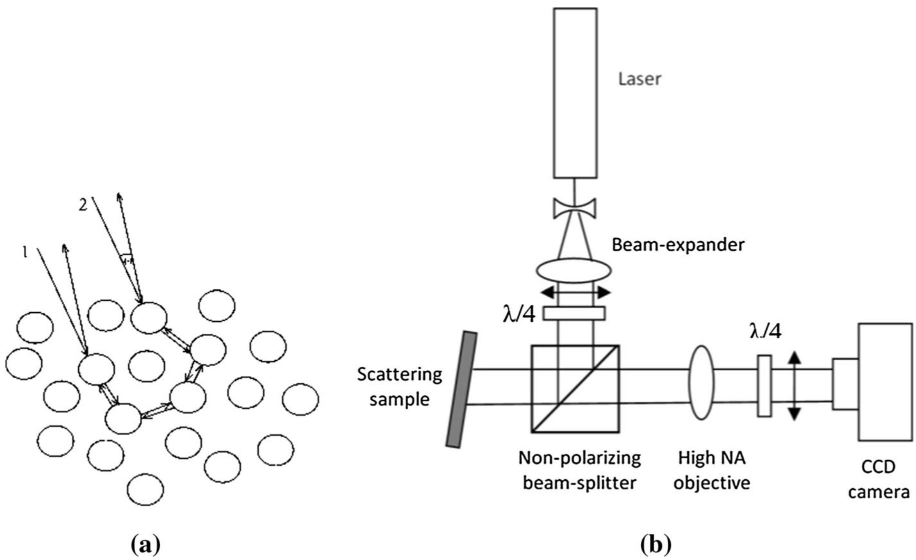

Fig. 2 **a** Coherent backscatter showing interference between counter-propagating light paths, **b** experimental setup

We have measured the backscattered light cone and determined the mean free path l of light in DCP structure by using the setup with circularly polarized light (Wiersma et al. 1995), schematically shown in Fig. 2b.

A He–Ne laser (633 nm) was used as a light source. The laser beam was expanded, and its polarization changed to circular, before entering the non-polarizing beam splitter. The spatial distribution of backscattered light is detected on a CMOS camera (15.1 mega pixel resolution, Canon EOS 50D), while speckle averaging was performed by vibrating the sample using electric motor. Clear backscattering signal is detected, obtained by averaging multiple camera exposures, as seen in Fig. 3 (down).

The value of the mean free path is calculated from angular width of the coherent backscattering peak, Fig. 3 (top). The full width at half maximum of the backscattering cone is W = 77 mrad, the value for the mean free path of light in DCP structure is $l = 0.9$ μm and $kl = 8.5$. This value indicates a weak localization regime (John 1984).

4 Conclusion

In conclusion, we investigated coherent backscatering by polysaccharide-based complex nanostructure. The structure, generated by holography, has pullulan nanoparticles, arranged in a random manner, and confined between DCP Bragg layers. We have measured the

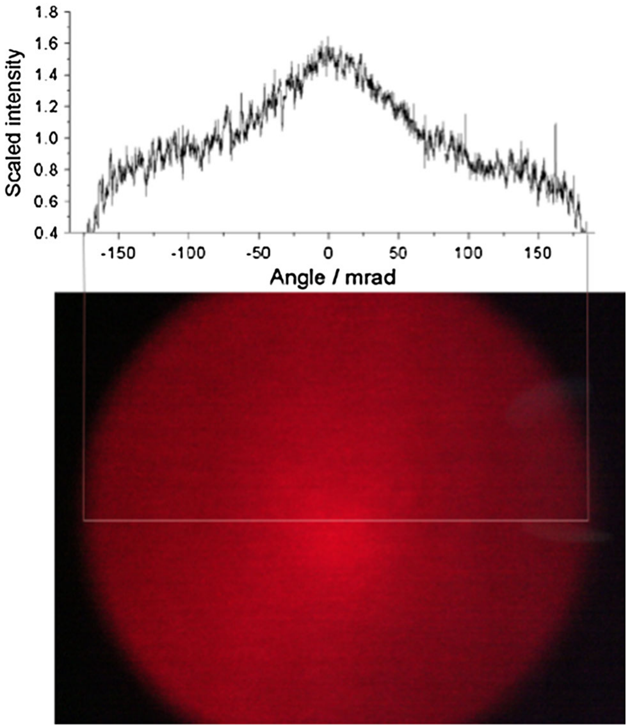

Fig. 3 Angular distribution of the backscattered light (*top*) and two dimensional image of backscattering obtained by averaging multiple camera exposures (*down*)

backscattered light cone and determined the mean free path of light in structure. It is verified experimentally that incident light is localized in disordered DCP photonic structures. The results indicate a weak localization regime.

Acknowledgments This work was funded by the Ministry of Education, Science and Technological Development of the Republic of Serbia, under Grants Nos. OI 171038 and III 45016.

References

Jendrzejewski, F., Müller, K., Richard, J., Date, A., Plisson, T., Bouyer, P., Aspect, A., Josse, V.: Coherent backscattering of ultracold atoms. Phys. Rev. Lett. **109**, 195302 (2012)

John, S.: Electromagnetic absorption in a disordered medium near a photon mobility edge. Phys. Rev. Lett. **53**, 2169–2172 (1984)

Jordan, T.M., Partridge, J.C., Roberts, N.W.: Disordered animal multilayer reflectors and the localization of light. J. R. Soc. Interface **11**, 20140948 (2014)

Li, X., Han, Y.: Tunable wavelength antireflective film by non-solvent-induced phase separation of amphiphilic block copolymer micelle solution. J. Mater. Chem. **21**, 18024–18033 (2011)

Liu, J., García, P.D., Ek, S., Gregersen, N., Suhr, T., Schubert, M., Mørk, J., Stobbe, S., Lodahl, P.: Random nanolasing in the Anderson localized regime. Nat. Nanotechnol. **9**, 285–289 (2014)

Pantelić, D., Savić, S., Jakovljević, D.: Dichromated pullulan as a novel photosensitive holographic material. Opt. Lett. **23**, 807–809 (1998)

Prajapati, V., Jani, G., Khanda, S.: Pullulan: an exopolysaccharide and its various applications. Carbohyd. Polym. **95**, 540–549 (2013)

Pratesi, F., Burresi, M., Riboli, F., Vynck, K., Wiersma, D.S.: Disordered photonic structures for light harvesting in solar cells. Opt. Exp. **21**, 460–468 (2013)

Savić, S., Pantelić, D., Jakovljević, D.: Real-time and postprocessing holographic effects in dichromated pullulan. Appl. Opt. **41**, 4484–4488 (2002)

Savić-Šević, S., Pantelić, D.: Dichromated pullulan diffraction gratings: influence of environmental conditions and storage time on their properties. Appl. Opt. **46**, 287–291 (2007)

Segev, M., Silberberg, Y., Christodoulides, D.: Anderson localization of light. Nat. Photon. **7**, 197–204 (2013)

Strangi, G., Ferjani, S., Barna, V., De Luca, A., Versace, C., Scaramuzza, N., Bartolino, R.: Random lasing and weak localization of light in dye-doped nematic liquid crystals. Opt. Exp. **14**, 7737–7744 (2006)

van Albada, M.P., Lagendijk, A.: Observation of weak localization of light in a random medium. Phys. Rev. Lett. **55**, 2692–2695 (1985)

van der Mark, M.B., van Albada, M.P., Lagendijk, A.: Light scattering in strongly scattering media: multiple scattering and weak localization. Phys. Rev. B **37**, 3575–3592 (1988)

Wiersma, D.: Disordered photonics. Nat. Photon. **7**, 188–196 (2013)

Wiersma, D.S., van Albada, M.P., Lagendijk, A.: An accurate technique to record the angular distribution of backscattered light. Rev. Sci. Instrum. **66**, 5473–5476 (1995)

Wiersma, D., Bartolini, P., Lagendijk, A., Righini, R.: Localization of light in a disordered medium. Nature **390**, 671–673 (1997)

Wolf, P.E., Maret, G.: Weak localization and coherent backscattering of photons in disordered media. Phys. Rev. Lett. **55**, 2696–2699 (1985)

Measuring temperature changes of butterfly's wing through deformation: a holographic approach

M. Simovic-Pavlovic[1,2], D. Grujic[2], P. Atanasijevic[3], D. Vasiljevic[2], B. Kolaric[2] and D. Pantelic[2]
[1]*University of Belgrade, Faculty of Mechanical Engineering, Belgrade, Serbia*
[2]*Institute of Physics, Belgrade, Serbia*
[3]*University of Belgrade, School of Electrical Engineering, Belgrade, Serbia*
e-mail: simovicmarina99@gmail.com

Natural colors originate from either chemical or physical properties or both combined. Colors of chemical origin are caused by pigments and dyes, while structural colors arise from light interference [1]. The latter, is due to the interaction of visible light, with nanometer-scale features of biophotonic structures. The Morpho (*Morpho didius*) butterfly's wing scale appeared as an example of the most beautiful biophotonic architecture. This particular wing is densely covered with iridescent scales (structures which look as micro-cantilevers). Furthermore, tiniest features of this biophotonic structure match the mean free path of air molecules at atmospheric pressure (approximately 100 nm), which is an essential condition to observe the photophoretic effect.

Thermal transport induced by laser radiation produces an additional thermophoretic force that deforms the wing scales [1]. Resulting deformation was monitored by real time digital holographic interferometry [2]. This deformation of wing scales can be used as a novel method of detecting low level thermal radiation. In our experiments we reached a temperature detection sensitivity of 2.9 mK, with the detection threshold of several $\mu J/cm^2$, depending on the wavelength [3].

ACKNOWLEDGEMENT: Here in this work, the concept of holographic detection of thermophoretic force is conceptually highlighted, experimentally confirmed and discussed.

REFERENCES
[1] C. Verstraete et al., J. Biophotonics 12, 1 (2019).
[2] D. Pantelić, D. Grujić, D. Vasiljević, J. Biomed. Opt. 19, 127005 (2014).
[3] D. Grujić et al., Opt. Express 26, 14143 (2018).

Graphene acoustic diaphragms

M. Spasenović[1], J. Mitrić[1], D. Abramović[2], N. Demoli[2], D. Grujić[1], D. Pantelić[1], D.Todorović[3,4]
[1]*Institute of Physics, University of Belgrade,*
Pregrevica 118, Belgrade, 11080, Serbia
[2]*Institute of Physics, Bijenička c. 46, PO Box 304, 10001 Zagreb, Croatia*
[3]*School of Electrical Engineering, University of Belgrade, Bulevar kralja Aleksandra 73, 11120 Belgrade, Serbia*
[4]*Dirigent Acoustics Ltd, Mažuranićeva 29/9, 11050 Belgrade, Serbia*
e-mail:spasenovic@ipb.ac.rs

Vibrating diaphragms have become an important component of acoustics technology, with nearly all commercial microphones and speakers of the past half a century relying on diaphragm vibration. Although few select materials (such as nickel and boPET) are predominantly used because of their favorable properties such as small mass density and large tensile strength, the rise of new materials with superior properties such as graphene demands an assessment of their potential use in acoustic diaphragms.

Here we evaluate various forms of graphene as an acoustic diaphragm material. We fabricate diaphragms from graphene paper and multilayer (~60 layers) CVD graphene and measure their response to acoustic stimuli either in capacitance mode, which most closely resembles actual use in electrostatic condenser microphones, or with digital holography, which allows for physical studies of diaphragm vibration modes [1]. We find that multilayer graphene diaphragms outperform traditional nickel membranes in terms of responsivity, up to 12 dB at audio frequencies [2]. For large-diameter (25 mm) diaphragms that can be made from graphene paper, we detect a rich array of acoustic vibration modes that point to the diaphragms' potential use in pressure sensing or for detection of weak acoustic signals in quiet environments.

Our findings are supported with numerical COMSOL calculations that also reveal that a thicker multilayer diaphragm made of 300 layers of CVD graphene would in theory sustain tension forces that allow ultrasonic reach. Hence we conclude that graphene diaphragms hold potential for miniature low-cost ultrasonic transducers that compete with current piezoelectric technology.

This work is supported by the Serbian MPNTR through project OI 171005. We thank the EU and the Republic of Serbia for financing through the Science – Industry Collaboration Program administered by the Innovation Fund.

REFERENCES

[1] N. Demoli and I. Demoli, Optics Express **13**, 4812 (2005).
[2] D. Todorović et al, 2D Materials **2**, 045013 (2015).

Digital holography of graphene oxide paper acoustic membranes

J. Mitrić[1], D. Abramović[2], D.Todorović[3,4],N. Demoli[2], M. Spasenović[1]
[1]*Graphene Laboratory (GLAB) of the Center for Solid State Physics and New Materials, Institute of Physics, University of Belgrade, Pregrevica 118, Belgrade, 11080, Serbia*
[2]*Institute of Physics, Bijenička c. 46, PO Box 304, 10001 Zagreb, Croatia*
[3]*School of Electrical Engineering, University of Belgrade, Bulevar kralja Aleksandra 73, 11120 Belgrade, Serbia*
[4]*Dirigent Acoustics Ltd, Mažuranićeva 29/9, 11050 Belgrade, Serbia*
e-mail: jmitric@ipb.ac.rs

Foil – like materials became almost unavoidable in industrial technology. Their applications are numerous, starting from protective and adhesive layers, chemical filters to electronic or optoelectronic components. Graphene oxide paper, as one of the most recent foil – like materials is made by assembly of individual graphene – oxide sheets. Its properties are superior compared to other materials when it comes to strength, stiffness and its macroscopic flexibility [1] which make it potentially a good candidate as a new material for vibrating membranes which are primary elements of every condenser microphone, loudspeaker and many other acoustic devices.

Here we report vibrating acoustic membranesmade of graphene oxide paper. We use digital holography in a quasi – Fourier configuration and time averaging to study the modal structures of the membranes [2, 3]. For comparison, we performed the same holographic measurements on membranes made of Mylar, aluminum, parafilm and different kinds of filter paper. We have found resonance frequencies and shapes of the vibrating modes for every tested material. We also calculated fundamental frequencies for every given material. Graphene oxide paper shows the richest modal behavior of all tested materials with multiple interesting and complex modes at frequencies between 20 Hz and 5 kHz.

This work is supported by the Serbian MPNTR through Projects OI 171005. We thank the EU and Republic of Serbia for financing through the Science – Industry Collaboration Program administered by the Innovation Fund.

REFERENCES

[1] D. A. Dikin, et al., Nature 448, 457 (2007).
[2] N. Demoli and I. Demoli, Optics Express 13, 4812 (2005).
[3] P. Picart, et al., Optics Letters 28, 1900 (2003).

8-6

Digital holography of graphene paper acoustic membranes and comparison to other paper – like materials

Jelena Mitrić,[1] Dušan Grujić,[2] Denis Abramović,[3] Iva Salom,[4]
Nazif Demoli,[3] Dejan Pantelić,[2] Dejan Todorović,[5] Marko Spasenović[2]
[1]School of Computing, University Union, Knez Mihailova 6, 11000 Belgrade, Serbia,
[2]Institute of Physics, University of Belgrade, Pregrevica 118, 11080 Belgrade, Serbia,
[3]Institute of Physics, Bijenička cesta 46, 10001 Zagreb, Croatia, [4]Institute Mihajlo Pupin, University of Belgrade, Volgina 15, 11060 Belgrade, Serbia, [5]Dirigent Acoustics Ltd, Mažuranićeva 29/9 11050, Belgrade, Serbia

Paper – like materials are becoming an important component of industrial technology. Their applications are numerous, starting from protective and adhesive layers, chemical filters to electronic or optoelectronic components. Graphene paper, as one of the youngest paper – like materials has favorable properties for all those applications, but also for novel applications in acoustics. Graphene paper is superior to other acoustic materials because it is lightweight, stiff, and has a large tensile strength. The aim of our project is to investigate the real – world potential of graphene – based acoustic membranes.

Here we report acoustic membranes made of graphene paper. We use time – averaged digital holography to study the vibrational modes of the membranes. Graphene paper shows a rich modal behavior in the audible part of the spectrum with multiple interesting and complex modes at frequencies between 40 Hz and 4 kHz. Numerical calculations confirm our experimental data, indicating a low pre – tension force (12.5 – 75 Nm^{-1}). For comparison, we performed the same holographic measurements on membranes made of Mylar polyester film, paraffin film, aluminum foil and different kinds of filter paper. We have found resonant modes for each tested membrane, with graphene paper showing the richest behavior. Our calculations indicate that more tightly pulled graphene paper membranes could be useful for applications in acoustics.

This work is supported by the Ministry of Education, Science and Technology of the Republic of Serbia. through Project OI 171005. We thank the EU and the Innovation Fund through the Collaborative Grant Scheme (Project 50038) administered by the Innovation Fund. We also thank Dirigent Acoustics Ltd for their continuing support.

FIZIČKI FAKULTET
UNIVERZITETA U BEOGRADU
Broj 2972010
Beograd, 18. 10. 2010. godine

Na osnovu člana 161. Zakona o opštem upravnom postupku i člana 4. Pravilnika o sadržaju i obliku obrazaca javnih isprava koje izdaju više škole, fakulteti i univerziteti, po zahtevu, Grujić Duana izdaje se sledeće

U V E R E N J E

GRUJIĆ (ŽIVOJIN) DUŠAN, rodjen 24. 02. 1984. godine u Kruševcu, R. Srbija upisana školske 2003/2004. godine na studijsku grupu **FIZIKA** smer **Primenjena fizika i informatika** položio je ispite predvidjene nastavnim planom i programom navedene Studijske grupe i diplomirao na Fizičkom fakultetu Univerziteta u Beogradu 13. oktobra 2010. godine, sa srednjom ocenom 8,14 (osam i 14/100) u toku studija i ocenom 10 (deset i 00/100) na diplomskom ispitu i time stekao visoku stručnu spremu (VII_1 stepen stručne spreme) i stručni naziv

DIPLOMIRANI FIZIČAR ZA PRIMENJENU FIZIKU I INFORMATIKU

Uverenje se izdaje na lični zahtev, a služi kao dokaz o završenoj visokoj stručnoj spremi (VII_1 stepen stručne spreme) do izdavanja diplome.

Uverenje je oslobodjeno plaćanja takse.

D E K A N
FIZIČKOG FAKULTETA

Prof. dr Ljubiša Zeković

РЕПУБЛИКА СРБИЈА

ФИЗИЧКИ ФАКУЛТЕТ
УНИВЕРЗИТЕТА У БЕОГРАДУ

ДИПЛОМА

О СТЕЧЕНОМ ВИСОКОМ ОБРАЗОВАЊУ

Грујић Животина Душан

РОЂЕН-А 24-II-1984. ГОДИНЕ У КРУШЕВЦУ, КРУШЕВАЦ СРБИЈА, УПИСАН-А 2003/2004. ГОДИНЕ, А ДАНА 13. ОКТОБРА 2010. ГОДИНЕ, ЗАВРШИО-ЛА ЈЕ СТУДИЈЕ НА ФИЗИЧКОМ ФАКУЛТЕТУ УНИВЕРЗИТЕТА У БЕОГРАДУ, НА СТУДИЈСКОЈ ГРУПИ ФИЗИКА СА ОПШТИМ УСПЕХОМ 8,14 (ОСАМ И 14/100) У ТОКУ СТУДИЈА И ОЦЕНОМ 10 (ДЕСЕТ) НА ДИПЛОМСКОМ ИСПИТУ.

НА ОСНОВУ ТОГА ИЗДАЈЕ МУ-ЈОЈ СЕ ОВА ДИПЛОМА О СТЕЧЕНОМ ВИСОКОМ ОБРАЗОВАЊУ И СТРУЧНОМ НАЗИВУ

ДИПЛОМИРАНИ ФИЗИЧАР ЗА ПРИМЕЊЕНУ ФИЗИКУ И ИНФОРМАТИКУ

РЕДНИ БРОЈ ИЗ ЕВИДЕНЦИЈЕ О ИЗДАТИМ ДИПЛОМАМА 2972010

У БЕОГРАДУ, 18. ОКТОБРА 2010. ГОДИНЕ

ДЕКАН

ПРОФ. ДР ЉУБИША ЗЕКОВИЋ

РЕКТОР

ПРОФ. ДР БРАНКО КОВАЧЕВИЋ

Република Србија
Универзитет у Београду
Физички факултет
Д.Бр.2018/8031
Датум: 17.10.2019. године

На основу члана 161 Закона о општем управном поступку и службене евиденције издаје се

УВЕРЕЊЕ

Грујић (Живојин) Душан, бр. индекса 2018/8031, рођен 24.02.1984. године, Крушевац, Република Србија, уписан школске 2019/2020. године, у статусу: самофинансирање; тип студија: докторске академске студије; студијски програм: Физика.

Према Статуту факултета студије трају (број година): три.
Рок за завршетак студија: у двоструком трајању студија.

Ово се уверење може употребити за регулисање војне обавезе, издавање визе, права на дечији додатак, породичне пензије, инвалидског додатка, добијања здравствене књижице, легитимације за повлашћену вожњу и стипендије.

Овлашћено лице факултета

Република Србија
Универзитет у Београду
Физички факултет
Д.Бр.2018/8031
Датум: 17.10.2019. године

На основу члана 161 Закона о општем управном поступку и службене евиденције издаје се

УВЕРЕЊЕ

Грујић (Живојин) Душан, бр. индекса 2018/8031, рођен 24.02.1984. године, Крушевац, Република Србија, уписан школске 2019/2020. године, у статусу: самофинансирање; тип студија: докторске академске студије; студијски програм: Физика.

Према Статуту факултета студије трају (број година): три.
Рок за завршетак студија: у двоструком трајању студија.

Ово се уверење може употребити за регулисање војне обавезе, издавање визе, права на дечији додатак, породичне пензије, инвалидског додатка, добијања здравствене књижице, легитимације за повлашћену вожњу и стипендије.

Овлашћено лице факултета

Република Србија
Универзитет у Београду
Физички факултет
Број индекса: 2018/8031
Датум: 17.10.2019.

На основу члана 29. Закона о општем управном поступку и службене евиденције издаје се

УВЕРЕЊЕ О ПОЛОЖЕНИМ ИСПИТИМА

Душан Грујић, име једног родитеља Живојин, рођен 24.02.1984. године, Крушевац, Република Србија, уписан школске 2018/2019. године на докторске академске студије, школске 2019/2020. године уписан на статус самофинансирање, студијски програм Физика, током студија положио је испите из следећих предмета:

Р.бр.	Шифра	Назив предмета	Оцена	ЕСПБ	Фонд часова**	Датум
1.	ДС15ФЛ6	Холографија и интерферометрија	8 (осам)	15	I:(8+0+0)	14.11.2018.
2.	ДС15ВО4	Нумеричке методе и симулације у квантној оптици	9 (девет)	15	II:(8+0+0)	14.11.2018.
3.	ДС15ФРНД1	Рад на докторату 1. део	П.	30	I:(0+0+12) II:(0+0+12)	
4.	ДС15ПФ7	Пројектовање оптичких система	10 (десет)	15	III:(8+0+0)	14.11.2018.
5.	ДС15ФЛ8	Макро и нано фотонске структуре у биофизици и оптичким комуникацијама	9 (девет)	15	III:(8+0+0)	01.07.2019.
6.	ДС15ФРНД2	Рад на докторату 2. део	П.	30	I:(0+0+12) II:(0+0+12)	
7.	ДС15ФРНД4	Рад на докторату 4. део	П.	15	VI:(0+0+20)	
8.	ДС15ФРНД3	Рад на докторату 3. део	П.	15	I:(0+0+20)	

* - еквивалентиран/признат испит.
** - Фонд часова је у формату (предавања+вежбе+остало).

Општи успех: 9,00 (девет и 00/100) , по годинама студија (8,50, 9,50, /).

Овлашћено лице факултета

ДОКТОРСКЕ СТУДИЈЕ

ПРЕДЛОГ ТЕМЕ ДОКТОРСКЕ ДИСЕРТАЦИЈЕ КОЛЕГИЈУМУ ДОКТОРСКИХ СТУДИЈА

Школска година 2018/2019

Подаци о студенту

Име: Душан

Презиме: Грујић

Број индекса: 8031/2018

Научна област дисертације: Фотоника и ласери

Подаци о ментору докторске дисертације

Име: Дејан

Презиме: Пантелић

Научна област: Фотоника и ласери

Звање: Научни саветник

Институција: Институт за физику

Предлог теме докторске дисертације

Наслов

Примена дигиталне холографије за детекцију инфрацрвеног зрачења на биофотонским структурама

Уз пријаву теме докторске дисертације Колегијуму докторских студија, потребно је приложити следећа документа:

1. Семинарски рад (дужине до 10 страница)
2. Кратку стручну биографију писану у трећем лицу једнине
3. Фотокопију индекса са докторских студија

		Потпис ментора	
Датум	29.08.2019	Потпис студента	

Мишљење Колегијума докторских студија

Након образложења теме докторске дисертације Колегијум докторских студија је тему

прихватио ☑ није прихватио ☐

Датум	Продекан за науку Физичког факултета
18.09.2019.	